Nano-Patterning by Diffraction Mask-Projection Laser Ablation

Marisa MÄDER, Klaus ZIMMER, Rico BÖHME, Thomas HÖCHE, Jürgen W. GERLACH and Bernd RAUSCHENBACH

Leibniz Institute of Surface Modification, Permoserstrasse 15, D-04318 Leipzig, Germany
E-mail: marisa.maeder@iom-leipzig.de

Nanostrcutures attached to a substrate promise optical and electronic applications. Moreover, applications for nanodots in various probing techniques are also aspired. So far, however, the fabrication process of most nanostructures is still very complex and often too costly for industrial use. An alternative, versatile, and fast process is laser ablation of a thin film using diffraction mask-projection. A pulsed excimer laser (wavelength 248 nm) is sent through a phase mask. The phase mask modulates the phase of the incident beam and provokes distinct diffraction maxima. Using a Schwarzschild reflection objective, the resulting interference pattern is demagnified and illuminates a thin film. When the ablation threshold of the underlying substrate clearly exceeds that of the thin film, the film is ablated at positions where the intensity is in excess of the ablation threshold of the film while the substrate remains unchanged. Different shapes of nanostructures can be fabricated this way. Applying about 1 J/cm^2, metal nanodots (gold, nickel and others) and gratings (titanium) were fabricated with this technique using a checkerboard mask. This method is in principle applicable to every combination of thin film and substrate material, as long as the ablation threshold of the substrate is high enough in comparison to the film ablation threshold.

DOI: 10.2961/jlmn.2008.01.0003
Keywords: Nano-patterning, laser ablation, phase mask, excimer laser, metal nano dots

1. Introduction

In this paper we will discuss the generation of substrate-bound dot- and grating-like metal nanostructures (size: about 100 nm, periodicity: about 700 nm) using diffraction mask-projection laser-ablation. Nanostructures of this shape and scale can find applications in a wide range. From using them as templates for catalytic nanowire growth to direct applications like optical data transfer or enhancing Raman signals by surface plasmons, various ideas are possible and suggested in literature (Henley et al. 2004, Henley et al. 2005). So far, however, structures with those dimensions are either difficult or costly to obtain. Diffraction mask-projection laser-ablation is a fast and convenient technique to create nanostructures like this. Another crucial advantage of the method is the possibility to impress a well defined order to the structures. While other groups obtained nanodots that were arranged statistically on the substrate (Henley, et al. 2005), it will be shown here that with our technique the structures can be decently arranged.

It will be demonstrated that the nanostructures that are bound to a substrate will form only under certain conditions. Micrographs of homogeneously arranged gold-dot arrays, created with mask-projection laser-ablation will be shown.

2. Experimental techniques

Diffraction mask-projection laser-ablation is a technique that can be divided into two basic processes. A thin film is deposited onto a substrate with established methods. Afterwards, the sample is illuminated by a laterally varying pattern of high laser intensity, possessing periodic distinct maxima and minima over a large homogeneous field. At positions where the intensity is high enough, the film is ablated and nanostructures of a well defined order remain on the substrate.

2.1 Thin film deposition

Thin films were produced by DC magnetron sputtering and electron beam evaporation with a film thickness ranging from 5 to 15 nm. Depending on the wetting behavior of the metal, continuous films were attained at different film thicknesses. Films were analyzed with a field emission gun scanning electron microscope (FEG-SEM) and film thickness was measured by x-ray reflectometry (XRR).

Substrate materials and metals were varied over a wide range. The following materials were used as substrates:

Material	Thermal conductivity (at 300 K) λ [W/Km]	Absorption coefficient (at 248 nm) α [x 10^6 1/m]	Orientation
Silicon	148	181	(100)
Sapphire	20	93	r: (1-102) c: (0001)
Silicon Carbide	350	13	(0001)
Fused Silica	1.4	≈ 0	amorphous

Table 1: Substrate materials and some of their important properties; thermal conductivity at 300 K, absorption coefficient at 248 nm and orientation

As film materials, nickel, aluminium, and iridium were evaporated by an electron beam, while gold, copper, and titanium were sputtered with a DC-magnetron.

Material	Melting / boiling point [K]	Thermal conductivity (at 300 K) [W/Km]	Reflectivity (at 248 nm)	Absorption coefficient x 10^6 (at 248 nm) [1/m]	Heat of fusion [kJ/kg] / evaporation [kJ/g]
Ir	2739 / 4701	150	0.56	119	137 / 2.9
Ti	1941 / 3560	22	0.23	61	389 / 8.9
Ni	1728 / 3186	91	0.45	106	301 / 6.6
Cu	1358 / 3200	400	0.37	90	205 / 4.7
Au	1337 / 3129	320	0.33	83	63 / 1.7
Al	934 / 2792	235	0.92	149	398 / 10.9

Table 2: Metals used as film material.

The materials show very different behavior under the same ablation conditions. Examples shown in the following were selected such that the underlying mechanisms can be elucidated at least in some important parts.

2.2 Mask projection

The diffraction mask-projection laser ablation technique takes advantage of the refractive and diffractive behavior of transmission phase masks. A pulsed KrF Excimer Laser (Lambda Physics, LPX220i, pulse duration: τ_L = 30 ns, wavelength: λ = 248 nm, repetition rate: 10 Hz) is sent through a diffractive phase mask (see Fig. 1), demagnified by a Schwarzschild-objective (demagnification: V = 15.29, numerical aperture: NA = 0.5, focal length: f = 13.41 mm) and focused onto a thin film on a substrate. The phase mask was manufactured by etching structures of well defined height into a fused silica wafer using lithographic methods (Höche et al. 2004, Höche et al. 2006).

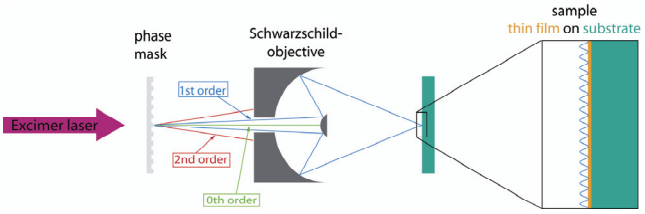

Fig. 1: Experimental setup for the diffraction mask-projection laser ablation technique

Height, size and periodicity of the mask structures are mainly determinate by the wavelength of the laser and the fixed parameters of the Schwarzschild-objective. The mask creates the common diffraction maxima of different orders (see Fig. 1). For our setup, the first order (±1 order) of diffraction is the only one that is used further.
This is achieved by a method especially designed for our setup. By varying the height of the structures in the phase mask, we can control enhancement or suppression of single orders of diffraction. Furthermore, the unwanted higher orders are cut out by the limiting aperture of the Schwarzschild-objective. The 0^{th} order is reflected by the first mirror of the objective.

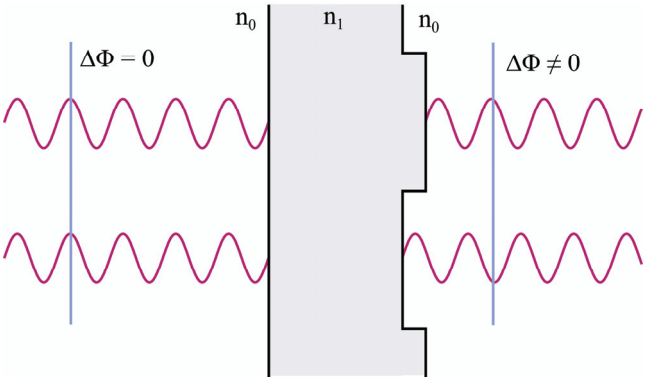

Fig. 2: Waves propagating through the refractive phase mask gain a phase shift relative to each other; ΔΦ: phase shift, n: index of refraction.

The enhancement or suppression of single order diffraction maxima is based on a principle similar to blazed gratings. Waves propagating through the refractive mask (index of refraction of fused silica at 248 nm: n_1 = 1.50855) will gain a phase shift if one of them must propagate a longer way through the mask. The retardation that is determined by the height of the structures in the mask must fulfill conditions that are either suppressing or enhancing the desired order. For the suppression of the 0^{th} order reflection (and therefore also for the enhancement of the $\pm 1^{st}$ order reflections) the phase shift must be π. The height h of the structures in the phase mask is then

$$h = \frac{\lambda}{2(n_1 - 1)}.$$

The geometrical arrangement can is indicated in Fig. 3.

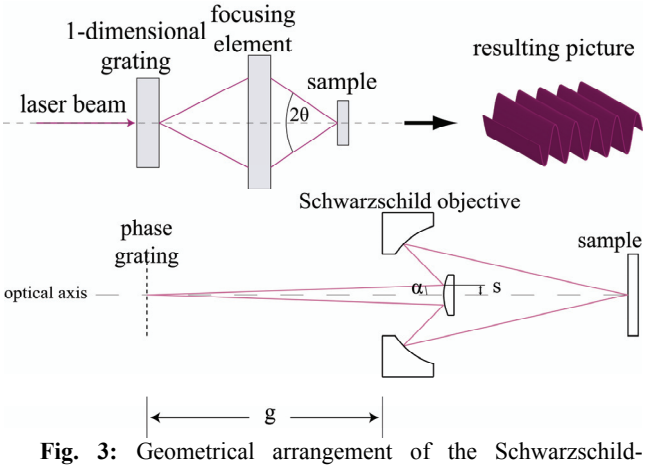

Fig. 3: Geometrical arrangement of the Schwarzschild-objective, the phase mask, and the sample.

The numerical aperture NA of the Schwarzschild-objective limits the angle θ, which determines the size of the resulting structures on the sample. Together with Bragg's law, the periodicity *a* of the mask structures can then be expressed as

$$a = \frac{2\lambda}{\sin\left[\arctan\frac{s}{g}\right]},$$

where s, g and a are shown in Fig. 2 and Fig. 3 and λ is the wavelength of the laser. For the Schwarzschild-objective with the parameters introduced before, this results in a periodicity of about 14 µm and a height of 244 nm for the structures etched into the phase mask. Therefore, the structures created on the sample possess a periodicity of about 700 nm. By using a different objective or changing *g*, the periodicity of the resulting structures can be varied. One of the main advantages of this technique is that the size of the structures that can be achieved is much smaller than predicted by the optical resolution of the Schwarzschild-objective.

The shape of the structures can be varied. So far, striped masks and a checkerboard mask were used.

3. Results and Discussion

The results can be split into two categories. The first is the process of ablation itself, and the second is the question what kind of influence the materials have on the formation of structures.

3.1 Process of ablation

Since the thin film can not be treated as bulk material and ablation is a process that does not take place in thermal equilibrium, a detailed theoretical description of the formation of the structures is difficult. The boundaries (air/film and film/substrate) included make a description even more difficult. Even though theoretical descriptions for thin film removal from different substrates already exist (Lee et al. 1999, Andrew et al. 1983, Veiko et al. 1980, Siegel et al. 1997), the process of nanostructure formation is more complex. Therefore an qualitative explanation of the formation process shall be given here.

By charging a very high energy density in short time scales into the film material, fast vaporization and liquid expulsion (Zhang et al. 1997, Veiko et al. 1980) takes place. The material is ripped off the substrate at places with sufficiently high intensity. The threshold fluence for ablation can be determined experimentally. If the threshold for ablation of the substrate is higher than the maximum of intensity that reaches the sample, the substrate remains unharmed in general. Choosing the film material such that the threshold for its ablation is just between the minima and maxima of intensity, the film should only be ablated at places where the intensity exceeds this threshold (see Fig. 4). In case of a sapphire substrate and an about 8-10 nm gold film, a fluence of about 1.0-1.5 J/cm^2 fulfills this condition. This way, structures will remain on the substrate within an ablation field of about 100x100 µm^2 in the present experiments.

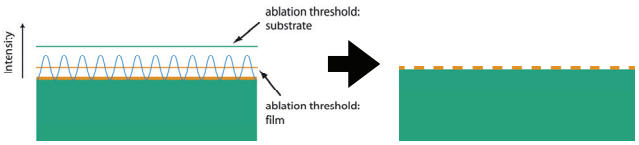

Fig. 4: Simplified sketch of the ablation process.

However, this is a very simplified model of the complex process. As described later, parameters like thermal conductivity of the substrate and the film as well as optical absorption behavior of both materials play crucial roles for the formation of the structures.

3.2 Results for different film/substrate combinations

During every experiment with the diffraction mask-projection laser ablation technique, the laser fluence was varied. The phase mask used for the experiments here, was a checkerboard. For different metals, substrates, and film thicknesses, one specific fluence turned out to give ideal conditions for the creation of nanostructures. The following FEG-SEM micrographs show some results for the same metal, i.e. gold, on different substrates.

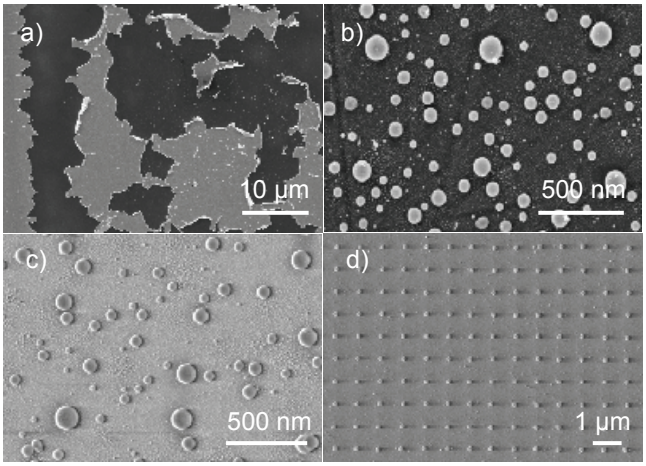

Fig. 5: Gold on different substrates after treatment by mask-projection laser ablation; initial film thicknesses: a) 19 nm Au on Si, b) 6 nm Au on SiC, c) 7 nm Au on SiO_2, d) 8 nm Au on Al_2O_3. The corresponding fluences were: 720 mJ/cm^2 for Si, 750 mJ/cm^2 for SiC, 165 mJ/cm^2 for SiO_2 and 1900 mJ/cm^2 for Al_2O_3.

As can be seen from the micrographs in Fig. 5, within the investigated parameter field, the diffraction mask-projection laser ablation technique only produces regularly arranged gold-nanodots on the sapphire substrate. This shows clearly that the substrate plays a major role for the formation of the nanostructures. The size of the nanodots is about 100 nm while the periodicity is 700 nm.

During the next step, the substrate remained the same for all experiments, i.e. fused silica, while the thin films consisted of different metals. Fig. 6 shows the best results for every metal that was used as a thin film.

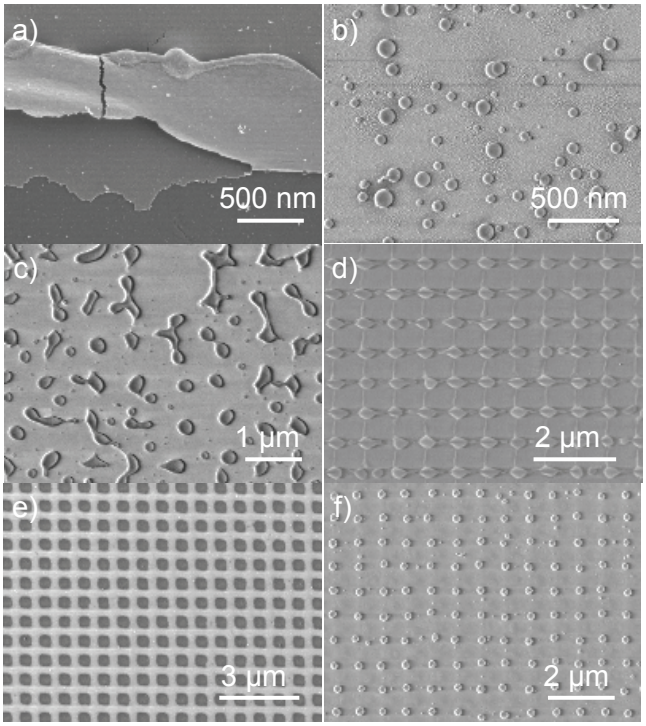

Fig. 6: Different metal films on fused silica after treatment with mask-projection laser ablation; a) 6 nm Ir, fluence: 20 mJ/cm^2 b) 6 nm Au, fluence: 165 mJ/cm^2 c) 10 nm Ni, fluence: 1200 mJ/cm^2 d) 7 nm Cu, fluence: 1200 mJ/cm^2 e) 5 nm Ti, fluence: 840 mJ/cm^2 f) 7 nm Al, fluence: 1200 mJ/cm^2

From those pictures, important details about the process of patterning by diffraction mask-projection laser-ablation can be derived. It seems that, using this method, a specific substrate-metal combination is necessary for the formation of nanostructures. Dots, however, will also form with other combinations than shown here (to be published). In the case of gold, for example, the substrate must not have an absorption coefficient that is about 0 if the thermal conductivity is also low (see Fig. 5c and table 2, fused silica). On the other hand, the thermal conductivity and absorption coefficient may not be too high either (see Fig. 5a and table 2, silicon). The important result that can be derived from the experiments shown here, is that for a successful formation of well ordered nanostructures a certain amount of heat energy (depending on the metal) must be provided by the substrate. This amount is – from the substrate's side – mainly determined by the thermal conductivity and the optical absorption behavior of the substrate. However, a quantitative description is yet to be found. Besides this, the results show that the optical absorption behavior of the metal also determines whether the structures are formed or not. The dependency, however, has to be investigated further.

The micrographs e) and f) in Fig. 6 show another interesting phenomenon. Generated under similar conditions (similar film thickness, similar laser fluence), the two metals behave totally different. Titanium builds a mesh bound to the substrate, while aluminium obviously merges to dot structures of minimized surface energy. Our assumption is that this process is mainly determined by the thermal conductivity and the surface tension of the individual metals. Aluminium, having a very high thermal conductivity can transport the heat within the short duration of illumination further than titanium that has a low thermal conductivity. The titanium is perhaps just ablated while the aluminium melts and diffuses to the point on the substrate which is heated least.

To see if the dimensions of the gold dots (i.e. height and diameter) can be controlled, experiments were done with different film thicknesses that were exposed to the same fluence (depending on the metal). The result is shown in Fig. 7. It turned out that both parameters strongly depend on the film thickness. By using a gold film only about 1 nm thicker than the first one, the dots could be enlarged by about 20 nm. As an explanation for this phenomenon we suggest that, using thicker films, more film material is available for the formation of dots. The structure of minimized surface energy is larger in every dimension.

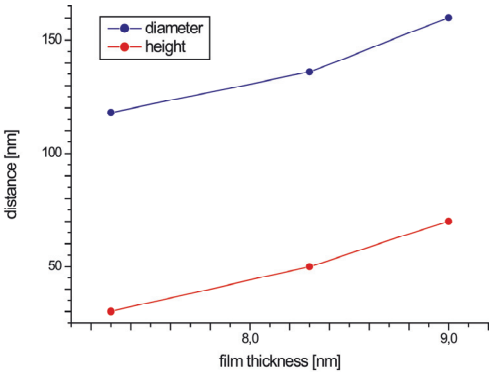

Fig. 7: Dependency of height and diameter of gold-dots on film thickness

4. Conclusions

It was shown that decently arranged nanostructures can be created by diffraction mask-projection laser-ablation of thin metal films. Process parameters, however, must fulfill specific conditions. To obtain successful formation of metal nanodots, the substrate must provide a certain amount of heat, that is restricted by the thermal conductivity and the absorption behavior of the substrate.

Diameter and height of the gold-dots can be controlled by varying the film thickness.

For other substrate-material combinations, the conditions where nanostructures form have yet to be found out. We showed, however, that the two most important parameters for the film as well as for the substrate material are the thermal conductivity and the optical absorption behavior.

Acknowledgment

Financial support by a Deutsche Forschungsgemeinschaft grant (# HO 1691/4-1) is gratefully acknowledged.

References

[1] Henley, S. J., Poa, C. H. P., Adikaari, A. D. T., Giusca, C. E., Carey, J. D. and Silva, S. R. P., 2004, *Appl. Phys. Lett.,* **84,** 4035-4037

[2] Henley, S. J., Carey, J. D. and Silva, S. R. P., 2005, *Phys. Rev. B,* **72,** 195408.

[3] Höche, T., Böhme, R., Gerlach, J.W., Frost, F., Zimmer, K., and Rauschenbach, B, 2004. *Nano Letters,* **4**, 895-897.
[4] Höche, T. Böhme, R., Gerlach, J. W., Rauschenbach, B., and Syrowotka, F., 2006, *Philos. Mag. Lett.* **86**, 661-667.
[5] Lee, S. K., Yoon, K. K., Whang, K. H. and Na, S. J., 1999, *Surf. Coat. Tech.,* **113,** 63-74.
[6] Andrew, J. E., Dyer, P. E., Greenough, R. D., and Key. P. H., 1983, *Appl. Phys. Lett.,* **43** (11), 1076-1078.
[7] Veiko, V. P., Metev, S. M., Kaidanov, A. I., Libenson, M. N., and Jakovlev, E. B., 1980, *J. Phys. D: Appl. Phys.,* **13,** 1565-1570.
[8] Siegel, J., Ettrich, K., Welsch, E., and Matthias, E., 1997, *Appl. Phys. A,* **64,** 213-218.
[9] Zhang, X. Chu, S. S., Ho, J. R., and Grigoropoulos, C. P., 1997, *Appl. Phys. A,* **64,** 545-552.

(Received: April 24, 2007, Accepted: November 7, 2007)